Article:
Muralidhar, S, Filia, A, Nsengimana, J et al. (11 more authors) (2019) Vitamin D-VDR signaling inhibits Wnt/beta-catenin-mediated melanoma progression and promotes anti-tumor immunity. Cancer Research, 79 (23). pp. 5986-5998. ISSN 0008-5472

https://doi.org/10.1158/0008-5472.CAN-18-3927

Role of vitamin D-VDR signaling in inhibition of Wnt/β-catenin mediated melanoma progression and promotion of anti-tumor immunity

Sathya Muralidhar[1,2], Anastasia Filia[3], Jérémie Nsengimana[1], Joanna Poźniak[1,4,5], Sally J. O'Shea[1,6,7], Joey M. Diaz[1], Mark Harland[1], Juliette A. Randerson-Moor[1], Jörg Reichrath[8], Jonathan P. Laye[1], Louise van der Weyden[9], David J. Adams[9], D. T. Bishop[1], Julia Newton-Bishop[1]

[1] University of Leeds School of Medicine, Leeds, UK
[2] Division of Molecular Pathology, The Institute of Cancer Research, UK
[3] Centre for Translational Research, Biomedical Research Foundation of the Academy of Athens, Athens, Greece
[4] Laboratory for Molecular Cancer Biology, VIB Center for Cancer Biology, KU Leuven, Leuven, Belgium
[5] Department of Oncology, KU Leuven, Leuven, Belgium
[6] Faculty of Medicine and Health, University College Cork, Cork, Ireland
[7] Mater Private Hospital Cork, Citygate, Mahon, Cork, Ireland
[8] Center for Clinical and Experimental Photodermatology, The Saarland University Hospital, Homburg, Germany
[9] Wellcome Sanger Institute, Wellcome Genome Campus, Hinxton, Cambridge, UK

Running title
Vitamin D-VDR signaling in primary melanoma prognosis

Keywords
Melanoma, vitamin D, VDR, Wnt/β-catenin, immune

Financial support
This work was funded by Cancer Research UK C588/A19167, C8216/A6129, and C588/A10721 and NIH CA83115. J. Poźniak, J.M.S. Diaz, and S. Muralidhar were funded by Horizon 2020 Research and Innovation Programme no. 641458 (MELGEN).

Correspondence
Professor Julia Newton-Bishop FMedSci
Professor of Dermatology,
Room 6.4 Clinical Sciences Building
Institute of Medical Research at St James's,
University of Leeds
+441132064668
J.A.Newton-Bishop@leeds.ac.uk

Conflict of interest statement
The authors have declared that no potential conflict of interest exists.

Abstract

1α,25-dihydroxyvitamin D_3 signals via the Vitamin D Receptor (VDR). Higher serum vitamin D is associated with thinner primary melanomas and better outcome, although a causal mechanism was not established. As melanoma patients commonly avoid sun exposure, and consequent vitamin D deficiency might worsen outcomes, we interrogated 703 primary melanoma transcriptomes to understand the role of vitamin D-*VDR* signalling and replicated the findings in TCGA metastases. *VDR* expression was independently protective for melanoma death in both primary and metastatic disease. High tumor *VDR* expression was associated with upregulation of pathways mediating anti-tumor immunity and correspondingly with higher imputed immune cell scores and histologically detected tumor infiltrating lymphocytes (TILs). High *VDR* expressing tumors had downregulation of proliferative pathways, notably Wnt/β-catenin signaling. Deleterious low *VDR* levels resulted from promoter methylation and gene deletion in metastases. Vitamin D deficiency (< 25 nmol/l ~ 10 ng/ml) shortened survival in primary melanoma in a *VDR*-dependent manner. *In vitro* functional validation studies showed that elevated vitamin D-VDR signaling inhibited Wnt/β-catenin signaling genes. Murine melanoma cells overexpressing *VDR* produced fewer pulmonary metastases than controls in tail vein metastasis assays. Vitamin D-VDR signaling contributes to controlling pro-proliferative/immunosuppresive Wnt/β-catenin signaling in melanoma and this is associated with less metastatic disease and stronger host immune responses. We report this as evidence of a causal relationship between vitamin D-VDR signaling and melanoma survival which should be explored as a therapeutic target in primary resistance to checkpoint blockade.

Statement of significance

This study highlights that the prognostic significance of vitamin D-VDR signaling in melanoma is associated with inhibition of Wnt/beta-catenin mediated tumour proliferation as well as enhanced anti-tumor host immune response.

Introduction

1α,25-dihydroxyvitamin D_3 is the ligand for the dimeric vitamin D receptor (VDR) and retinoid X receptor (RXR): ligand-receptor binding facilitates transcription of target genes containing the vitamin D response element (VDRE) (1). The physiological effect of the vitamin D-*VDR* signaling axis is often target tissue-specific (2).

The association of low serum 25-hydroxyvitamin $D_{2/3}$ levels (henceforth referred to as vitamin D) with higher cancer incidence has been reported (3) but the significance of the association has been debated (4). Extensive *in vitro* evidence however indicates an anti-proliferative role of vitamin D, with $1,25(OH)_2$ vitamin D_3 treatment shown to induce expression of pro-apoptotic genes and anti-proliferative genes in prostate (5), breast (6), colon (7) squamous cell carcinoma and leukaemia cells (8, 9).

We have previously reported that higher serum vitamin D levels at recruitment were associated with lower AJCC stage and better melanoma specific survival (MSS) in the Leeds Melanoma Cohort (LMC) (10). This was subsequently verified in 5 additional studies (11-15), which collectively indicate a significant role for vitamin D-VDR signaling in melanoma progression.

The unique dataset used in this study was derived from 703 formalin-fixed paraffin-embedded (FFPE) primary melanomas, from the LMC, a population-based and extensively annotated cohort with a long follow-up (10). Tumor-derived transcriptomic data, clinical, histopathological and whole-genome copy number alteration (CNA) data were jointly analysed to assess the pan-genome effects of vitamin D-*VDR* signaling and to determine the processes most associated with this pathway. Importantly, these findings were replicated in TCGA metastatic melanomas and then functionally validated using *in vitro* and *in vivo* experiments.

Materials and methods

The Leeds Melanoma Cohort (LMC) tumor transcriptome

LMC tumor transcriptome processing was described previously (16)(accession no. EGAS00001002922). Briefly, tumor samples were taken from formalin fixed paraffin embedded (FFPE) primary melanomas and RNA was extracted to generate whole genome gene expression data (Illumina DASL HT12.4 array). Background correction and quantile normalisation were applied; singular value decomposition was used to assess the confounding factors which were subsequently adjusted out. Participants in the LMC gave written informed consent; the study was conducted in accordance to international ethical guidelines (Declaration of Helsinki) and was approved by the national ethics committee (MREC 1/03/57 and PIAG3-09(d)/2003).

Measurement of serum vitamin D at diagnosis

For 554 of the 703 participants with transcriptomic data, 25-hydroxyvitamin vitamin D_2 and D_3 (nmol/L) was measured as described previously (10) and adjusted for season (see Supplementary Methods).

TCGA melanoma dataset

TCGA metastatic melanoma data (n=365 samples) such as transcriptomic (RNA-Seq), clinical, methylation and copy number data were downloaded from cBioPortal (http://www.cbioportal.org/). The same statistical tests and software/packages were used to analyse Leeds and TCGA data.

Statistical analyses

Association of VDR expression with clinical variables: univariate and multivariate linear regression were used to test the association between *VDR* and AJCC stage, mitotic number, tumor site, age and sex.

Association of VDR expression with MSS: univariate and multivariate Cox proportional hazards models were used to test the prognostic effect of *VDR* expression level after adjusting for AJCC stage (7^{th} Edition), tumor mitotic number, tumor site and TILs. For this analysis *VDR* expression was on the continuous log2 scale, meaning that Hazard Ratio (HR) per *VDR* unit corresponds to change in hazard when expression is doubled.

VDR copy number changes in the LMC tumors

Copy number profiles were estimated from NGS output from sequenced DNA samples from a subset of LMC tumors (n=276, 39%) as described (17). Gistic2.0 was used to identify *VDR* copy number estimates (see Supplementary Methods).

Whole-transcriptome correlation with *VDR*

Linear regression analysis and Benjamini-Hochberg multiple testing correction (False Discovery Rate- FDR) was used to test the correlation between the expression of each gene and *VDR* in the tumors. Genes with FDR<0.05 and |Reg Coef|>0.2 (Reg Coef- Regression coefficient) were plotted in a volcano plot (R function: 'plot') and used for functional enrichment analysis.

Since VDR is expressed by keratinocytes (18), a *FLG2*-adjusted whole-transcriptome correlation with *VDR* was additionally performed (Fillagrin family member 2: *FLG2* being a maker of keratinocyte differentiation). This sensitivity analysis was conducted to account for any bias in *VDR* expression which might have originated from keratin-rich melanoma subsets, which have been previously reported (19-21).

Functional enrichment analyses

The 'Gene set/mutation analysis' feature of ReactomeFIViz (22) was used to identify significantly enriched pathways (Benjamini-Hochberg FDR <0.05, from hypergeometric test) from a given input gene list.

VDR-binding regions

The genomic regions identified as having VDR-binding peaks across 6 tissue types (23) were downloaded as BED files. Additionally, genomic regions known to contain the VDR-binding motif were downloaded from Motifmap (as BED files). In both cases, genes associated with genomic regions were identified using GREAT 3.0.0 (24): 'Basal plus extension' approach was used with Human GRCh37 assembly, whole genome as background regions and the gene regulatory domain set to ±20 kb upstream and ±400 kb distal. The genes which mapped to these regions ('region-

gene associations') were exported and their overlap with *VDR*-correlated genes in the LMC (at FDR<0.05) was assessed.

VDR expression across Lund and TCGA molecular phenotypes

Nearest centroid method (21) was used to classify the LMC tumors into TCGA and Lund molecular melanoma phenotypes (see Supplementary Methods). Differential *VDR* expression across these subgroups was tested with the Mann-Whitney test.

Imputed Immune scores

As described by Pozniak et al (25). Briefly, 28 immune cell scores were calculated as mean expression of genes pertaining to an immune cell type, after deducting genes identified as potentially non-immune cell specific, from the initial immune gene signature described by Angelova et al. Correlation analysis of each immune cell score with *VDR* expression was conducted.

Expression of *VDR* and response to checkpoint blockade

VDR expression was compared between responders and non-responders in two published albeit small transcriptomic data sets: i) 38 patients treated with PD-1 blockade (26) and ii) 40 patients treated with CTLA4 blockade (27). Both studies used pretreatment biopsies. Fold change was computed as ratio of mean *VDR* expression in responders to non-responders

Vitamin D-*VDR* subgroup analysis

X-tile (28) was used to identify patient subgroups with the most contrasted survival profiles (melanoma-specific) based on their tumor *VDR* expression in the LMC. This approach was trained in randomly selected 2/3 of the samples and validated in the remaining 1/3. The cut-points defining patient subgroups in terms of percentiles were applied to the TCGA metastatic melanoma dataset for replication.

The identified *VDR* groups were further stratified based on participants' serum vitamin D levels at recruitment (season-adjusted) in the LMC. Clinically defined vitamin D deficiency is generally considered to be <25 nmol/L (29), with recent evidence defining vitamin D deficiency able to compromise bone health as ≤30nmol/L (30). Thus, in the LMC dataset, serum vitamin D levels <25nmol/L and ≥25nmol/L were classified as 'deficient' and 'sufficient'.

Vitamin D treatment of human melanoma cells

SK-MEL-28 and MeWo cells (courtesy of Professor Alan Melcher, Leeds CRUK cell line bank) were authenticated using the PowerPlex 16 System (Promega, USA), cultured, treated with 1,25 $(OH)_2$ vitamin D_3 (Supplementary Methods), collected at different time points, RNA extracted and used to generate gene expression profiles (HG-U133 plus 2.0 array, Affymetrix). Genes differentially expressed in vitamin D-treated versus control cells were identified at each time point (FDR<0.10) and were used for functional enrichment using Reactome FIViz.

Generation of VDR-B16BL6 and control-B16BL6 cells

B16BL6 cells (chosen owing to lowest endogenous *VDR* expression among B16 strains, estimated from transcriptomic data by Dr Martin del Castillo- personal communication) were purchased from the M. D. Anderson Cancer Center Cell Line Core facility. Cells were screened for the presence of mycoplasma and mouse pathogens (at Charles River Laboratories, USA) before culturing. Early passage B16BL6 cells were cultured and transfected with murine *VDR* cDNA (synthesised by GeneArt™) or empty backbone plasmid to generate the VDR-B16BL6 (clones V1, V2) and control-B16BL6 (clones C1, C2) cells respectively (Supplementary Methods), verified by Western blot and qRT-PCR.

In vivo tail-vein metastasis assay

Though subcutaneous B16 models have bene used to demonstrate the role of NK cells in host responses to melanoma, we adopted the tail-vein model based on successful demonstration by the group of a role for effector T-cells and NK cells in B16 pulmonary metastases studies (31) and other reports of a role for T-cells in B16 melanoma cells (32-34). The care and use of all mice in this study were in accordance with the UK Animals in Science Regulation Unit's Code of Practice for the Housing and Care of Animals Bred, or Used for Scientific Purposes, the Animals (Scientific Procedures) Act 1986 Amendment Regulations 2012, and all procedures were performed under a UK Home Office Project license, which was reviewed and approved by the Sanger Institute's Animal Welfare and Ethical Review Body.

Housing and husbandry conditions were as described previously (31) and mice were maintained on Mouse Breeders' Diet (Laboratory Diets, 5021-3) throughout the study. V1, V2, C1 and C2 cells (detailed above) were tail-vein administered to 6-10 week old sex-matched wildtype (C57BL/6NTac) mice (10^4 cells in 0.1mL PBS). After 21 days, mice were humanely sacrificed and their lungs macroscopically examined to determine the number of metastatic deposits in all 5 lobes ('met count'). Lungs were formalin fixed, processed and embedded in paraffin wax blocks, from which consecutive 5μm sections were cut. and used for H&E and CD3 staining. H&E sections were digitally scanned (Leica Aperio AT2) and total metastatic area ('met area' μm^2) was calculated as the total area of all metastatic deposits, across all 5 lung lobes using Aperio Imagescope (Leica Biosystems). CD3+ lymphocytes were estimated as described in Supplementary Methods.

Wnt/β-catenin signaling in *VDR*-B16BL6 and control-B16BL6 cells

cDNA from V1, V2, C1 and C2 cells were analysed using a RT-PCR array of 84 mouse Wnt/β-catenin pathway genes (see Supplementary Methods). Relative expression was calculated using the Delta-Delta CT method, normalized to average Ct of the 5 housekeeping genes provided in the array. Fold change (FC) of the *VDR*-B16BL6 clones relative to control-B16BL6 clones was calculated as follows: $FC_{V1(or)V2} = 2^{(-\Delta\Delta Ct)_{V1(or)V2}}$ where $\Delta\Delta Ct_{V1(or)V2} = \Delta Ct_{V1(or)V2} - \Delta Ct_{avg(C1 \& C2)}$.

Results

VDR expression is independently protective for melanoma death in the LMC primary and TCGA metastatic melanomas

VDR expression was significantly lower in tumors of higher AJCC stage, higher mitotic rate and tumors on the trunk and sun protected sites (compared to tumors on the head) (Univariate analysis, Table 1) in the 703 LMC primaries. In multivariate analysis, lower *VDR* expression was independently associated with higher mitotic rate (*P*=0.001) and tumor site (*P*=0.001 for tumors of trunk compared to those on head), with borderline significance for higher stage (*P*<0.06) (Table 1).

Higher tumor *VDR* expression was protective for melanoma death independent of stage, tumor mitotic rate, tumor site and histologically reported TILs (HR for melanoma death=0.80, *P*=0.008, Table 1). Though *VDR* expression correlated significantly with other members of the NR1IL family such as *LXRB*, *FXR1, FXR2* and *PXR* expressions (Supplementary Table 1), it remained significantly prognostic after adjusting for the expression of those genes (adjusted HR for melanoma death=0.77, *P*=0.001).

Since VDR forms heterodimers with RXR and RXRγ signalling has been reported to drive epithelial/mesenchymal transition and invasion in melanoma, we tested the prognostic effect of the expression of genes coding for RXR receptors. In the LMC, *VDR* did not correlate significantly with *RXRγ* (Supplementary Table 1) and the prognostic significance of *VDR* expression was independent of the expression of *RXRα, RXRβ* and *RXRγ* (adjusted HR for melanoma death=0.75, *P*=0.0001)

Immunohistochemistry of LMC primary melanomas revealed that VDR expression was predominantly in tumor (rather than immune) cells (representative image in Supplementary Figure 1, quantified in Supplementary Table 2).

In the TCGA metastatic melanomas (n=353), higher *VDR* expression was protective for death (Overall survival HR=0.82, *P*=0.03).

Tumor *VDR* expression is associated variably with CNAs and promoter methylation in primary and metastatic melanomas

In the LMC primary melanomas, *VDR* expression showed a weak positive correlation with *VDR* copy number, which failed to reach statistical significance (*P*=0.12, Figure 1A). However, in the TCGA metastatic melanomas, *VDR* expression was lowest in

tumors with *hemizygous* deletion compared to those with 'no changes/neutral' (*P*=0.01) and was significantly higher in tumors with 'gain' (*P*=0.007) and 'high-level amplifications' (*P*<0.00001) (Figure 1B). *VDR* copy number was more frequently reduced in distant metastases compared to regional lymph node metastases (*P*=0.015, Figure 1C). Concomitantly, the TCGA data also showed progressively reduced *VDR* expression from primary to lymph node then distant metastases (Figure 1D). *VDR* expression was significantly and inversely correlated with *VDR* promoter methylation (*P*=0.0001, Figure 1E) in TCGA metastases.

VDR correlates positively with genes enriched for immune-related pathways and negatively with proliferation-related pathways in LMC primary and TCGA metastases

In the LMC, an agnostic whole-transcriptome correlation analysis identified genes positively (n=2025) and negatively (n=3408) correlated with *VDR* (Figure 2). The negatively correlated genes were enriched for proliferation-related pathways such as mitotic prometaphase, Wnt signaling, mitochondrial translation, TCA cycle, and cadherin signaling (Figure 2, Supplementary Table 3). By contrast, the positively correlated genes were enriched for immune-related pathways such as cytokine-cytokine receptor interaction, TNF, IFNγ, IL12-mediated, NFκB and chemokine signaling (Figure 2, Supplementary Table 4). *VDR*-correlated genes remained largely unchanged after *FLG2*-adjustment (Methods, Supplementary Table 5), indicating that confounding from epidermal sampling is unlikely.

We assessed if the *VDR*-correlated genes in the LMC were known to have a VDR-binding site. Tuoresmaki et al. previously reported 54 non-overlapping genomic VDR-binding regions recurrent in 6 tissue types, based on meta-analysis of VDR ChIP-Seq data (23). We mapped the 54 genomic binding regions to be associated with 73 genes (GREAT, sMethods), of which 43 genes (58%) were among the significant *VDR*-correlated genes in the LMC. Alternatively, 60% of genes mapped to genomic regions containing the VDR-binding motif (identified by Motifmap, see Methods) also correlated significantly with *VDR* in the LMC.

In the TCGA metastatic melanomas, *VDR* correlated negatively with genes enriched for: ECM organization, cadherin signaling, eukaryotic translation initiation, TGFβ and VEGFR1 signaling; and positively with: NFκB, TNF, IFNα/β, IFNγ, IL12-

mediated, TCR and chemokine signaling in naïve CD4 T-cells pathways (Supplementary Tables 6 and 7). The majority overlapped with those observed in LMC primaries.

Tumor *VDR* expression is associated with reported melanoma phenotypes, imputed immune cell scores and reduced Wnt/β-catenin signaling

The LMC primaries were classified based on previously described melanoma molecular phenotypes (20, 35) (Supplementary Methods). The TCGA signature (20) classified the 703 LMC melanomas into Immune (n=192), Keratin (n=247) and *MITF*-low (n=150) subtypes. *VDR* expression was significantly higher in the Keratin and Immune subtypes compared to the *MITF*-low subtype (P=1.1x10^{-6}) (Figure 3A). The Lund signature (35) classified tumors into High-immune (n=173), Normal-like (n=198), Pigmentation (n=222) and Proliferative (n=83) subtypes. *VDR* expression was significantly higher in High-immune subtype compared to the poorer prognosis Proliferative (P= 7.5x10^{-8}) and Pigmentation subtypes (P=6x10^{-13}) (Figure 3B).

VDR expression correlated positively with 25 of the 26 immune cell scores (Supplementary Table 8) of which the strongest correlation (Correlation coefficient>0.30) was with Dendritic cells, MDSCs, neutrophils, central memory CD4, NK, Th1, Th2 and T-cells (Figure 3C). Concordantly, *VDR* expression was significantly lower in tumors with 'absent' immune infiltrate compared to tumors with 'non-brisk' (P=0.02) and 'brisk' immune infiltrate (P=0.004) (Figure 3D), according to histopathological scores which were available for 601 (86%) of the LMC melanomas.

We previously reported an immunologically "cold" tumor subtype in the LMC (Consensus Immunome Cluster 4, CIC4) with increased β-catenin signaling, reduced imputed immune scores for cytotoxic, T cell and activated dendritic cells (aDC) and expression of genes coding for checkpoint molecules (16). *VDR* expression was lowest in that tumor subtype (Figure 3E), which was concordant with the agnostic correlation analysis identifying Wnt/β-catenin as the pathway most strongly associated with low immune signals in both LMC primary and TCGA metastatic melanomas.

To compare *VDR* expression with response to immunotherapy, we used previously published therapy-response datasets (26, 36). *VDR* expression did not vary significantly between responders (n=15) and non-responders (n=13) to anti-PD-

1 therapy (*P*=0.27), nor to anti-CTLA4 treatment (P=0.12) in a dataset of responders and (n=13) non-responders (n=22) (Supplementary Figure 2), although in the latter, *VDR* expression was 1.35 times higher in responders compared to non-responders (Fold Change= 1.35).

Deficient levels of serum vitamin D are associated with more melanoma deaths within the context of *VDR* expression

The 703 LMC primary melanomas were stratified into 3 groups using a survival-based stratification approach (X-tile, see Methods). *VDR* expression thresholds which best predicted differential survival identified the following groups: 17% with the lowest *VDR* expression (low-*VDR* group, n=119), 17% of tumors with highest *VDR* expression (high-*VDR* group, n=119) and middle 66% (intermediate-*VDR* group, n=465) having the worst, best and intermediate survival respectively (*P*= 5.2×10^{-8}, Figure 4A-B). This was replicated in the TCGA metastatic melanomas (n=353) using the same *VDR* expression percentiles (*P*=0.03, Figure 4C-D).

Amongst the three *VDR* groups: deficient serum vitamin D levels (<25nmol/L) were associated with poorer prognosis compared to sufficient vitamin D levels ($\geq$25nmol/L) in the intermediate-*VDR* group (HR=1.73, *P*=0.02), but not in the low-*VDR* (*P*=0.66) or high-*VDR* (*P*=0.55) groups (Figure 4E). The deleterious association with vitamin D deficiency was therefore apparent within the context of *VDR* expression. Intermediate-*VDR* group participants with deficient vitamin D were characterised by higher Breslow thickness (*P*=0.02), higher frequency of pathologist-reported vascular invasion (*P*=0.01) and AJCC stage II tumors (compared to stage I: *P*=0.01), when compared to those with sufficient vitamin D. An agnostic whole-transcriptome analysis identified no gene significantly differentially expressed (at FDR<0.10) between participants with deficient or sufficient vitamin D in the intermediate-*VDR* group. However, among the pathways that correlated significantly with *VDR* (Figure 2), the following were significantly underexpressed in participants with vitamin D sufficiency: NK cell mediated cell killing (*P*=0.02), IL12 (*P*=0.03) and TCR signaling on naïve CD4 and CD8 signaling (*P*=0.05).

Vitamin D treatment and increased *VDR* expression inhibit Wnt/β-catenin pathway and melanoma cell growth *in vitro* and *in vivo*

We functionally validated our findings from the LMC primary and TCGA metastatic melanomas, where high *VDR*-expressing tumours (with active vitamin D-VDR signaling) had better survival and reduced expression of proliferative pathways, in particular the Wnt/β-catenin signaling. The human melanoma cell lines SK-MEL-28 and MeWo treated with 1,25 $(OH)_2$ vitamin D_3 showed reduced proliferation post-treatment (Figure 5A). At 24 and 48 hours post-treatment, *VDR* expression was significantly upregulated while Wnt signaling and ECM organization genes were among the top downregulated pathways in both cell lines. The pathways upregulated in both cell lines at both time points were: MAPK, IFNα/β, TGFβ and TLR signaling (Figure 5B).

In a second functional validation model, the *in vivo* metastatic potential of murine melanoma B16BL6 cells overexpressing VDR ("VDR-B16BL6 cells") was compared to control cells expressing low/no VDR ("control-B16BL6 cells") (Supplementary Figure 3). Mice injected with VDR-B16BL6 cells developed significantly lower pulmonary metastatic load (metastatic area and metastases count) compared to those dosed with control-B16BL6 cells (P<0.04), with comparable results from both clones in two independent experiments (pooled analyses from 2 experiments represented in Figure 5C). Differential expression of Wnt/β-catenin pathway genes between VDR-B16BL6 and control-B16BL6 was compared using a pre-formatted qRT-PCR-based array. Of the 84 Wnt/β-catenin genes tested, 62 genes had lower expression (fold change <1, of which 26 had fold change ≤0.5) in both VDR clones compared to control clones (Figure 5D). Twelve genes had increased expression (fold change>1, none with fold change≥2) in both VDR clones.

In comparing the tumor immune infiltrate: though the number of CD3+ cells/100 mm^2 met area was not statistically significantly higher in mice injected with VDR-B16BL6 cells (P=0.11, compared to control-B16BL6 cells), there was a trend for increased CD3+ immune infiltrate (Supplementary Figure 4).

Collectively, both models provide causal evidence that elevated vitamin D-VDR signaling in melanomas cells inhibits Wnt/β-catenin signalling and tumor proliferation.

Discussion

Melanoma is one of the most immunogenic malignancies: increased lymphocytic infiltration in both primaries (37, 38) and metastases (39) is associated with improved outcomes (16, 21) and melanoma responses to immune checkpoint blockade are high (40, 41). However, dampened immune responses and therapeutic resistance attributed to oncogenic pathways such as Wnt/β-catenin signaling (16, 42) mean that only 58% of stage IV melanoma patients have significant benefit. Identification of factors that boost anti-tumor immunity is required to improve outcomes.

Low vitamin D levels are associated with thicker, poorer-prognosis primary melanomas (11), and lower VDR expression is associated with melanoma progression (43, 44) but neither causality nor the mechanistic basis has been established. In this report, we demonstrate that vitamin D-VDR signaling is protective for melanoma death at least in part through inhibition of Wnt/β-catenin signaling, impacting on melanoma proliferation and anti-tumor immune response.

We report that *VDR* expression was significantly lower in advanced tumors in the LMC primary melanomas. Importantly, high *VDR* expression was independently protective of melanoma death after adjusting for AJCC stage, mitotic rate and TILs. Survival benefit was replicated in the TCGA metastatic tumors, highlighting the significance of vitamin D-VDR signaling in both primary and metastatic melanoma progression. This protective effect of *VDR* was independent of the expression of other *NR1L* family genes, despite reports of integrated activity between nuclear receptors (45). In assessing factors which could control *VDR* expression, *VDR* copy number was not significantly associated with expression in LMC primaries. However, distant metastases (which have worse prognosis) had lower *VDR* copy number compared to regional lymph node metastases in the TCGA, suggesting a progression-associated genomic loss of *VDR.* Low *VDR*-expressing metastatic tumors from TCGA were also more likely to be hypermethylated, consistent with previous reports of the epigenetic control of *VDR* expression (46). Despite the progressive deletion of the *VDR* locus with tumor progression in metastatic disease, the data suggest that therapeutic manipulation of vitamin D-VDR signaling could have adjuvant therapeutic benefit in primary disease where we saw little evidence of *VDR* deletion.

An agnostic correlation analysis revealed that *VDR* expression was strongly positively correlated with immune-related pathways and negatively correlated with proliferation-associated pathways in LMC primaries and TCGA metastases. An additional sensitivity analyses adjusting for *FLG2* expression, produced no significant changes in the correlated pathways, indicating that artefact from keratinocyte-rich tumor populations was unlikely. *VDR* expression was higher in 'brisk' immune-infiltrated primaries compared to tumors with no immune infiltrate, which is in agreement with a previous report of a smaller immunohistochemical study (43) and is an independent validation of the transcriptomic imputation of immune infiltration. 58% of the genes within reported genomic VDR-binding regions (identified from VDR ChIP-Seq data as well as VDR-binding motif) were found to correlate with tumour *VDR* expression in the LMC. This is consistent with direct transcriptional control by the VDR transcription factor for a proportion of differentially expressed genes.

Validation using published prognostic melanoma molecular phenotypes (16, 35) revealed that *VDR* expression was significantly higher in high-immune subtypes compared to proliferative subtypes, consistent with the view that the prognostic significance of *VDR* is associated with increased immune and decreased proliferative signaling. We also assessed if *VDR* preferentially correlated with a particular immune cell type, which was previously uncharacterised in primary melanomas. However, *VDR* was strongly positively correlated with all imputed immune cell scores: we have previously reported simultaneous upregulation of adaptive and innate immunity in good prognosis primary melanomas (16). Furthermore, the pro-immune effect of vitamin D-VDR signaling was supported by strong positive correlation of *VDR* with genes involved in pathways such as extracellular matrix organization, TNFα, NFκB, IFNγ and IL-12-mediated signaling.

In comparing pre-treatment gene expression between responders and non responders to immunotherapy, *VDR* expression was higher in responders to anti-CTLA4 (FC=1.35), albeit not statistically significant (P=0.12) in this very small data set. Though data from these immunotherapy studies did not support *VDR* expression as a biomarker of response, we posit that the data sets available to explore *VDR* as a biomarker were insufficient to properly explore this possibility.

Wnt/β-catenin signaling was among the top negatively-correlated pathways with *VDR* in the LMC and TCGA melanomas, concordant with reports of vitamin D-VDR-

mediated inhibition of Wnt/β-catenin signaling in colon cancer (47). We further explored this relationship and report that *VDR* expression was lowest in previosuly reported subset of tumors characterized by high-Wnt/β-catenin expression, reduced immune infiltrate and high mortality (16). Collectively, our findings support the hypothesis that, as in colon cancer, some of the effects of vitamin D-*VDR* siganling in melanoma are mediated by inhibition of Wnt/β-catenin signaling.

Vitamin D deficiency (≤25nmol/L, ~10ng/ml) was associated with worse prognosis only in participants with intermediate-*VDR* expression (albeit the majority). Though an agnostic analysis identified no significant transcriptomic differences associated with vitamin D in this subgroup, there was some evidence for paradoxically reduced expression of immune-associated pathways with higher vitamin D levels in a candidate gene expression analysis. The reported associations between vitamin D and the immune system are numerous and complex. The findings of this study are therefore not inconsistent with the view that vitamin D deficiency should be avoided but that high levels would not necessarily be beneficial to all patients.

The lack of a protective effect of higher vitamin D levels in participants with low-*VDR* tumors was not unexpected as low receptor expression could preclude effective signaling despite ligand sufficiency. A lack of benefit in the high-*VDR* tumors was more surprising and we postulate that this could reflect receptor saturation as reported in other NHR family receptors (48) or a ligand-independent effect of VDR, which has been described in other cancers (49, 50).

In functional validation, the observed vitamin D-treatment induced reduction in cell proliferation is concordant with previous reports (51). However, the pan-trasncriptome-based findings that vitamin D treatment of human melanoma cell lines promotes *VDR* expression and inhibition of pro-tumor pathways including the Wnt/β-catenin pathway, is novel. Furthermore, elevated *VDR* expression in murine melanoma cells decreased their *in vivo* metastatic potential the expression of key Wnt/β-catenin genes, some of which (*Dkk1* and *Sfrp2*) have previously been shown to be inhibited by VDR (52), but not in melanomas. Interestingly, the 'classic' non-canonical Wnt ligands *Wnt5a, Wnt5b, Wnt10a, Wnt7* and *Wnt11* were also downregulated by VDR. This finding is of significance because Wnt5a (and some other non-canonical Wnt ligands) affect cell motility and invasion and is implicated in

worse melanoma prognosis (53). Thus, the findings functionally validate the trasncriptome-derived evidence for the inverse association between VDR and Wnt/β-catenin signalling.

We report a trend towards increased T cell infiltration of lung metastases produced by *VDR*-expressing B16BL6 melanoma cells, although this did not reach statistical significance. Rejection of B16 derivative melanoma cell lines *in vivo* requires both NK and T-cells, and in the pulmonary metastasis model, NK cell derived IFN-gamma is important but T-cells also exert important anti-tumour activity (32-34, 54-57). The lack of statistically significant reduction in T cell numbers does not exclude the possibility that T-cells are more active and/or that NK cell recruitment and activity is also modified. To this effect, further analyses of T cell and NK recruitment and activity following VDR manipulation is warranted using both the subcutaneous and metastatic B16 models.

This study reports that vitamin D-VDR signaling bestows a prognostic benefit for melanoma patients by inhibiting Wnt/β-catenin signaling and increasing immune cell infiltration. These findings also suggest that activating vitamin D-VDR signaling has the potential to enhance anti-tumor immunity in an adjuvant setting. Notably, our findings suggest that vitamin D deficiency (<25nmol/L) is deleterious for melanoma survival rather than that high levels are protective. As melanoma is causally related to intense sun burn (58), sun avoidance is frequently recommended to patients in follow up. Our data suggest a causal relationship between reduced vitamin D-VDR signaling and therefore, as sun exposure is the dominant vitamin D source in most populations, simultaneous avoidance of vitamin D deficiency is important health advice.

Acknowledgements

Our grateful thanks to the participants who gave of their time and their very blood. Also to the research nurses and technicians who collected the data over many years: Susan Leake, Susan Haynes, Birute Karpavicius, Paul Affleck, Kairen Kukalizch, Linda Whitaker, Sharon Jackson, Edwina Gerry, Elaine Fitzgibbon, Clarissa Nolan, Saila Waseem, Yvonne Taylor, Pauline Brunyee, Paul King, Tracy Lee, Samira Lobo and Minttu Polso. To Jo Gascoyne and May Chan who provided critical support in managing the complex data set. We thank Dr. Robert Salmond, University of Leeds for his guidance and access to cell culture facilities and Professor Graham Cook for immunological insights. We acknowledge the advice and assistance of Kenneth MacLennan, Consultant Professor of Tumour Pathology at Leeds Teaching Hospitals NHS Trust in reviewing immunohistochemistry sections.

We thank Dr. James Hewinson (Experimental Cancer Genetics group, Wellcome Sanger Institute) for his valuable assistance to the *in vitro* transfection experiments. We thank Dr. Martin del Castillo for aiding in the choice of appropriate cell line for the *in vitro* and *in vivo* experiments.

References

1. Haussler MR, Jurutka PW, Mizwicki M, and Norman AW. Vitamin D receptor (VDR)-mediated actions of 1alpha,25(OH)(2)vitamin D(3): genomic and non-genomic mechanisms. *Best practice & research Clinical endocrinology & metabolism.* 2011;25(4):543-59.
2. Campbell FC, Xu H, El-Tanani M, Crowe P, and Bingham V. The yin and yang of vitamin D receptor (VDR) signaling in neoplastic progression: operational networks and tissue-specific growth control. *Biochem Pharmacol.* 2010;79(1):1-9.
3. Garland CF, Garland FC, Gorham ED, Lipkin M, Newmark H, Mohr SB, et al. The role of vitamin D in cancer prevention. *Am J Public Health.* 2006;96(2):252-61.
4. Autier P, Boniol M, Pizot C, and Mullie P. Vitamin D status and ill health: a systematic review. *Lancet Diabetes Endocrinol.* 2014;2(1):76-89.
5. Guzey M, Luo J, and Getzenberg RH. Vitamin D3 modulated gene expression patterns in human primary normal and cancer prostate cells. *Journal of cellular biochemistry.* 2004;93(2):271-85.
6. Swami S, Raghavachari N, Muller UR, Bao YP, and Feldman D. Vitamin D growth inhibition of breast cancer cells: gene expression patterns assessed by cDNA microarray. *Breast Cancer Res Treat.* 2003;80(1):49-62.
7. Wood RJ, Tchack L, Angelo G, Pratt RE, and Sonna LA. DNA microarray analysis of vitamin D-induced gene expression in a human colon carcinoma cell line. *Physiol Genomics.* 2004;17(2):122-9.
8. Suzuki T, Tazoe H, Taguchi K, Koyama Y, Ichikawa H, Hayakawa S, et al. DNA microarray analysis of changes in gene expression induced by 1,25-dihydroxyvitamin D3 in human promyelocytic leukemia HL-60 cells. *Biomed Res.* 2006;27(3):99-109.
9. Wang TT, Tavera-Mendoza LE, Laperriere D, Libby E, MacLeod NB, Nagai Y, et al. Large-scale in silico and microarray-based identification of direct 1,25-dihydroxyvitamin D3 target genes. *Molecular endocrinology.* 2005;19(11):2685-95.
10. Newton-Bishop JA, Beswick S, Randerson-Moor J, Chang YM, Affleck P, Elliott F, et al. Serum 25-hydroxyvitamin D3 levels are associated with breslow thickness at presentation and survival from melanoma. *Journal of clinical oncology : official journal of the American Society of Clinical Oncology.* 2009;27(32):5439-44.
11. Timerman D, McEnery-Stonelake M, Joyce CJ, Nambudiri VE, Hodi FS, Claus EB, et al. Vitamin D deficiency is associated with a worse prognosis in metastatic melanoma. *Oncotarget.* 2017;8(4):6873-82.
12. Fang S, Sui D, Wang Y, Liu H, Chiang YJ, Ross MI, et al. Association of Vitamin D Levels With Outcome in Patients With Melanoma After Adjustment For C-Reactive Protein. *Journal of clinical oncology : official journal of the American Society of Clinical Oncology.* 2016;34(15):1741-7.
13. Wyatt C, Lucas RM, Hurst C, and Kimlin MG. Vitamin D deficiency at melanoma diagnosis is associated with higher Breslow thickness. *PloS one.* 2015;10(5):e0126394.
14. Gambichler T, Bindsteiner M, Hoxtermann S, and Kreuter A. Serum 25-hydroxyvitamin D serum levels in a large German cohort of patients with melanoma. *The British journal of dermatology.* 2013;168(3):625-8.

15. Saiag P, Aegerter P, Vitoux D, Lebbe C, Wolkenstein P, Dupin N, et al. Prognostic Value of 25-hydroxyvitamin D3 Levels at Diagnosis and During Follow-up in Melanoma Patients. *J Natl Cancer Inst.* 2015;107(12):djv264.
16. Nsengimana J, Laye J, Filia A, O'Shea S, Muralidhar S, Pozniak J, et al. beta-Catenin-mediated immune evasion pathway frequently operates in primary cutaneous melanomas. *The Journal of clinical investigation.* 2018;128(5):2048-63.
17. Filia A, Droop A, Harland M, Thygesen H, Randerson-Moor J, Snowden H, et al. High-Resolution Copy Number Patterns From Clinically Relevant FFPE Material. *Sci Rep.* 2019;9(1):8908.
18. Bikle DD. Vitamin D and the skin: Physiology and pathophysiology. *Rev Endocr Metab Disord.* 2012;13(1):3-19.
19. Lauss M, Nsengimana J, Staaf J, Newton-Bishop J, and Jonsson G. Consensus of Melanoma Gene Expression Subtypes Converges on Biological Entities. *J Invest Dermatol.* 2016;136(12):2502-5.
20. The Cancer Genome Atlas Network. Genomic Classification of Cutaneous Melanoma. *Cell.* 2015;161(7):1681-96.
21. Nsengimana J, Laye J, Filia A, Walker C, Jewell R, Van den Oord JJ, et al. Independent replication of a melanoma subtype gene signature and evaluation of its prognostic value and biological correlates in a population cohort. *Oncotarget.* 2015;6(13):11683-93.
22. Wu G, and Stein L. A network module-based method for identifying cancer prognostic signatures. *Genome biology.* 2012;13(12):R112.
23. Tuoresmaki P, Vaisanen S, Neme A, Heikkinen S, and Carlberg C. Patterns of genome-wide VDR locations. *PloS one.* 2014;9(4):e96105.
24. McLean CY, Bristor D, Hiller M, Clarke SL, Schaar BT, Lowe CB, et al. GREAT improves functional interpretation of cis-regulatory regions. *Nat Biotechnol.* 2010;28(5):495-501.
25. Pozniak J, Nsengimana J, Laye JP, O'Shea SJ, Diaz JMS, Droop AP, et al. Genetic and Environmental Determinants of Immune Response to Cutaneous Melanoma. *Cancer Res.* 2019.
26. Hugo W, Zaretsky JM, Sun L, Song C, Moreno BH, Hu-Lieskovan S, et al. Genomic and Transcriptomic Features of Response to Anti-PD-1 Therapy in Metastatic Melanoma. *Cell.* 2017;168(3):542.
27. Van Allen EM, Miao D, Schilling B, Shukla SA, Blank C, Zimmer L, et al. Genomic correlates of response to CTLA-4 blockade in metastatic melanoma. *Science.* 2015;350(6257):207-11.
28. Camp RL, Dolled-Filhart M, and Rimm DL. X-tile: a new bio-informatics tool for biomarker assessment and outcome-based cut-point optimization. *Clinical cancer research : an official journal of the American Association for Cancer Research.* 2004;10(21):7252-9.
29. SACN TSACoN. *SACN recommendations on vitamin D*. 2016.
30. Shah S, Chiang C, Sikaris K, Lu Z, Bui M, Zebaze R, et al. Serum 25-Hydroxyvitamin D Insufficiency in Search of a Bone Disease. *J Clin Endocrinol Metab.* 2017;102(7):2321-8.
31. van der Weyden L, Arends MJ, Campbell AD, Bald T, Wardle-Jones H, Griggs N, et al. Genome-wide in vivo screen identifies novel host regulators of metastatic colonization. *Nature.* 2017;541(7636):233-6.

32. Curran MA, Montalvo W, Yagita H, and Allison JP. PD-1 and CTLA-4 combination blockade expands infiltrating T cells and reduces regulatory T and myeloid cells within B16 melanoma tumors. *Proceedings of the National Academy of Sciences of the United States of America.* 2010;107(9):4275-80.
33. Ryu MS, Woo MY, Kwon D, Hong AE, Song KY, Park S, et al. Accumulation of cytolytic CD8+ T cells in B16-melanoma and proliferation of mature T cells in TIS21-knockout mice after T cell receptor stimulation. *Exp Cell Res.* 2014;327(2):209-21.
34. Xu D, Gu P, Pan PY, Li Q, Sato AI, and Chen SH. NK and CD8+ T cell-mediated eradication of poorly immunogenic B16-F10 melanoma by the combined action of IL-12 gene therapy and 4-1BB costimulation. *International journal of cancer.* 2004;109(4):499-506.
35. Jonsson G, Busch C, Knappskog S, Geisler J, Miletic H, Ringner M, et al. Gene expression profiling-based identification of molecular subtypes in stage IV melanomas with different clinical outcome. *Clinical cancer research : an official journal of the American Association for Cancer Research.* 2010;16(13):3356-67.
36. Van Allen EM, Miao D, Schilling B, Shukla SA, Blank C, Zimmer L, et al. Genomic correlates of response to CTLA-4 blockade in metastatic melanoma. *Science.* 2015;350(6257):207-11.
37. Oble DA, Loewe R, Yu P, and Mihm MC, Jr. Focus on TILs: prognostic significance of tumor infiltrating lymphocytes in human melanoma. *Cancer Immun.* 2009;9:3.
38. Clemente CG, Mihm MC, Jr., Bufalino R, Zurrida S, Collini P, and Cascinelli N. Prognostic value of tumor infiltrating lymphocytes in the vertical growth phase of primary cutaneous melanoma. *Cancer.* 1996;77(7):1303-10.
39. Erdag G, Schaefer JT, Smolkin ME, Deacon DH, Shea SM, Dengel LT, et al. Immunotype and immunohistologic characteristics of tumor-infiltrating immune cells are associated with clinical outcome in metastatic melanoma. *Cancer Res.* 2012;72(5):1070-80.
40. Haanen JB. Immunotherapy of melanoma. *EJC Suppl.* 2013;11(2):97-105.
41. Wolchok JD, Chiarion-Sileni V, Gonzalez R, Rutkowski P, Grob JJ, Cowey CL, et al. Overall Survival with Combined Nivolumab and Ipilimumab in Advanced Melanoma. *N Engl J Med.* 2017;377(14):1345-56.
42. Spranger S, Bao R, and Gajewski TF. Melanoma-intrinsic beta-catenin signalling prevents anti-tumour immunity. *Nature.* 2015;523(7559):231-5.
43. Brozyna AA, Jozwicki W, and Slominski AT. Decreased VDR expression in cutaneous melanomas as marker of tumor progression: new data and analyses. *Anticancer research.* 2014;34(6):2735-43.
44. Slominski AT, Brozyna AA, Zmijewski MA, Jozwicki W, Jetten AM, Mason RS, et al. Vitamin D signaling and melanoma: role of vitamin D and its receptors in melanoma progression and management. *Lab Invest.* 2017;97(6):706-24.
45. Long MD, and Campbell MJ. Pan-cancer analyses of the nuclear receptor superfamily. *Nucl Receptor Res.* 2015;2.
46. Saccone D, Asani F, and Bornman L. Regulation of the vitamin D receptor gene by environment, genetics and epigenetics. *Gene.* 2015;561(2):171-80.
47. Aguilera O, Pena C, Garcia JM, Larriba MJ, Ordonez-Moran P, Navarro D, et al. The Wnt antagonist DICKKOPF-1 gene is induced by 1alpha,25-dihydroxyvitamin D3 associated to the differentiation of human colon cancer cells. *Carcinogenesis.* 2007;28(9):1877-84.

48. Bennesch MA, and Picard D. Minireview: Tipping the balance: ligand-independent activation of steroid receptors. *Molecular endocrinology.* 2015;29(3):349-63.
49. Skorija K, Cox M, Sisk JM, Dowd DR, MacDonald PN, Thompson CC, et al. Ligand-independent actions of the vitamin D receptor maintain hair follicle homeostasis. *Molecular endocrinology.* 2005;19(4):855-62.
50. Trivedi T, Zheng Y, Fournier PGJ, Murthy S, John S, Schillo S, et al. The vitamin D receptor is involved in the regulation of human breast cancer cell growth via a ligand-independent function in cytoplasm. *Oncotarget.* 2017;8(16):26687-701.
51. Spath L, Ulivieri A, Lavra L, Fidanza L, Carlesimo M, Giubettini M, et al. Antiproliferative Effects of 1alpha-OH-vitD3 in Malignant Melanoma: Potential Therapeutic implications. *Sci Rep.* 2017;7:40370.
52. Cianferotti L, and Demay MB. VDR-mediated inhibition of DKK1 and SFRP2 suppresses adipogenic differentiation of murine bone marrow stromal cells. *Journal of cellular biochemistry.* 2007;101(1):80-8.
53. Katoh M. WNT/PCP signaling pathway and human cancer (review). *Oncol Rep.* 2005;14(6):1583-8.
54. Takeda K, Nakayama M, Sakaki M, Hayakawa Y, Imawari M, Ogasawara K, et al. IFN-gamma production by lung NK cells is critical for the natural resistance to pulmonary metastasis of B16 melanoma in mice. *J Leukoc Biol.* 2011;90(4):777-85.
55. van der Weyden L, Karp NA, Swiatkowska A, Adams DJ, and Speak AO. Genome wide in vivo mouse screen data from studies to assess host regulation of metastatic colonisation. *Sci Data.* 2017;4:170129.
56. Umeshappa CS, Zhu Y, Bhanumathy KK, Omabe M, Chibbar R, and Xiang J. Innate and adoptive immune cells contribute to natural resistance to systemic metastasis of B16 melanoma. *Cancer Biother Radiopharm.* 2015;30(2):72-8.
57. Taylor A, Rothstein D, and Rudd CE. Small-Molecule Inhibition of PD-1 Transcription Is an Effective Alternative to Antibody Blockade in Cancer Therapy. *Cancer Res.* 2018;78(3):706-17.
58. Chang YM, Barrett JH, Bishop DT, Armstrong BK, Bataille V, Bergman W, et al. Sun exposure and melanoma risk at different latitudes: a pooled analysis of 5700 cases and 7216 controls. *Int J Epidemiol.* 2009;38(3):814-30.

Table 1

	Univariate			Multivariate		
Correlation of tumour *VDR* expression with	Regression Coefficient	Std. Error	P-value	Regression Coefficient	Std. Error	P-value
Age (per year)	-0.005	0.002	0.04	-0.003	0.002	0.14
Sex						
Females[B]						
Males	-0.18	0.06	0.003	-0.09	0.06	0.16
AJCC Stage						
Stage I[B]						
Stage II	-0.17	0.07	0.012	-0.12	0.07	0.08
Stage III	-0.25	0.09	0.009	-0.18	0.09	0.06
Mitotic rate						
<1 mitoses/mm^2 tumor[B]						
>=1mitoses/mm^2 tumor	-0.23	0.06	0.0004	-0.20	0.06	0.001
Tumor site						
Head[B]						
Limbs	-0.04	0.10	0.63	-0.11	0.10	0.28
Trunk	-0.35	0.10	0.001	-0.36	0.10	0.001
Rare (sun protected sites)	-0.44	0.12	0.001	-0.38	0.13	0.003
	Univariate			**Multivariate***		
	Hazard Ratio	Std Error	P-value	Hazard Ratio	Std Error	P-value
Effect of tumour *VDR* expression on MSS (per unit expression)	0.75	0.05	0.0001	0.80	0.06	0.008

Table 1: Association of tumor *VDR* expression with clinicopathological variables and MSS in the 703 LMC participants. [B]Baseline group used for comparison with relevant groups. *Multivariate survival analysis was adjusted for AJCC stage, mitotic rate, tumor site and tumor immune infiltrate. MSS: Melanoma Specific Survival. Regression Coefficient and P-value from linear regression.

Figure legends

Figure 1. Association of *VDR* expression with copy number and methylation
A) Correlation of *VDR* expression with copy number in 276 LMC primaries B) *VDR* expression across categorical copy number estimates from TCGA melanoma metastases: -1 (hemizygous deletion), 0 (no change), 1(gain) and 2 (high-level amplification) C) *VDR* median copy number in regional lymph node and distant metastases in the TCGA melanomas D) *VDR* expression in distant, regional lymph node metastases and primary tumours in the TCGA dataset E) *VDR* expression and promoter methylation in TCGA metastases.

Figure 2. Whole-transcriptome correlations with *VDR* expression Volcano plot of genes correlated significantly (FDR<0.05) positively (regression coefficient>0.2, green dots) and negatively (regression coeffficent <-0.2, red dots) with *VDR* expression in the LMC data; top 25 pathways enriched for each gene list are listed in adjoining tables (left for negative, right for positive correlates). FDR: Benjamini-Hochberg False Discovery Rate.

Figure 3. Association of *VDR* expression with measures of immune response
A-B) Comparison of *VDR* expression between LMC samples classified into Lund and TCGA prognostic molecular phenotypes C) Correlation of *VDR* expression with imputed immune cell scores whose correlation coefficient>0.3 D) *VDR* expression across pathologist-graded TILs in the whole tumor FFPE section (P-values from the Student t-test) E) Heatmap depicting expression of *VDR* expression (top bar), cytotoxic, T cell and aDC scores, expression of genes coding for checkpoint molecules, and expression of Wnt/β-catenin siganling genes across the 6 consensus immunome clusters (CICs) reported previously (16).

Figure 4. Vitamin D and *VDR* subgroup analysis in the Leeds Melanoma Cohort dataset A) prognosis-based stratification of 703 LMC tumors into low-, intermediate- and high-*VDR* tumor groups identified using X-tile B) Kaplan-Meier curves showing the differential melanoma-specific survival in those groups C-D) Replication of the 3 *VDR*-groups and their association with overall survival in TCGA metastases. E) Melanoma-specific survival of 6 vitamin D-*VDR* subgroups produced by stratification of 3 *VDR* groups by low (<25nmoles/L) or high (≥25nmoles/L) serum vitamin D levels for winter season. All P-values from the Cox model.

Figure 5. Functional validation using *in vitro* and *in vivo* models A) Relative proliferation of vitamin D-treated human melanoma cell lines SK-MEL-28 and MeWo: 24, 48, 72 and 144 hours after treatment, compared to ethanol-treated cells (control). B) Pathways enriched in genes upregulated (green bars) or down-regulated (red bars) in response to vitamin D treatment of SK-MEL-2828 and MeWo cell lines at 24 and 48 hours post-treatment C) Pulmonary metastatic loads in control-B16BL6 (clones C1 and C2) and VDR-B16BL6 (clones V1 and V2) obtained from the tail vein metastasis assay. Met count: macroscopic counts of metastases, met area: total microscopic metastatic area (μm^2) in mice lung sections, N-number of mice/group. Inset: represenative H&E scanned images of metastases-harboring pulmonary lobes D) qRT-PCR array-derived expression of Wnt/β-catenin pathway genes in VDR-B16BL6 cells (V1 and V2) (FC=fold change relative to control-B16BL6 cells). Highlighted in red: genes with a FC<0.5 for both VDR-B16BL6 clones V1 and V2.

Table 1

	Univariate			Multivariate		
Correlation of tumour *VDR* expression with	Regression Coefficient	Std. Error	P-value	Regression Coefficient	Std. Error	P-value
Age (per year)	-0.005	0.002	0.04	-0.003	0.002	0.14
Sex						
Females[B]						
Males	-0.18	0.06	0.003	-0.09	0.06	0.16
AJCC Stage						
Stage I[B]						
Stage II	-0.17	0.07	0.012	-0.12	0.07	0.08
Stage III	-0.25	0.09	0.009	-0.18	0.09	0.06
Mitotic rate						
<1 mitoses/mm^2 tumor[B]						
>=1mitoses/mm^2 tumor	-0.23	0.06	0.0004	-0.20	0.06	0.001
Tumor site						
Head[B]						
Limbs	-0.04	0.10	0.63	-0.11	0.10	0.28
Trunk	-0.35	0.10	0.001	-0.36	0.10	0.001
Rare (sun protected sites)	-0.44	0.12	0.001	-0.38	0.13	0.003
	Univariate			**Multivariate***		
	Hazard Ratio	Std Error	P-value	Hazard Ratio	Std Error	P-value
Effect of tumour *VDR* expression on MSS (per unit expression)	0.75	0.05	0.0001	0.80	0.06	0.008

Figure 1

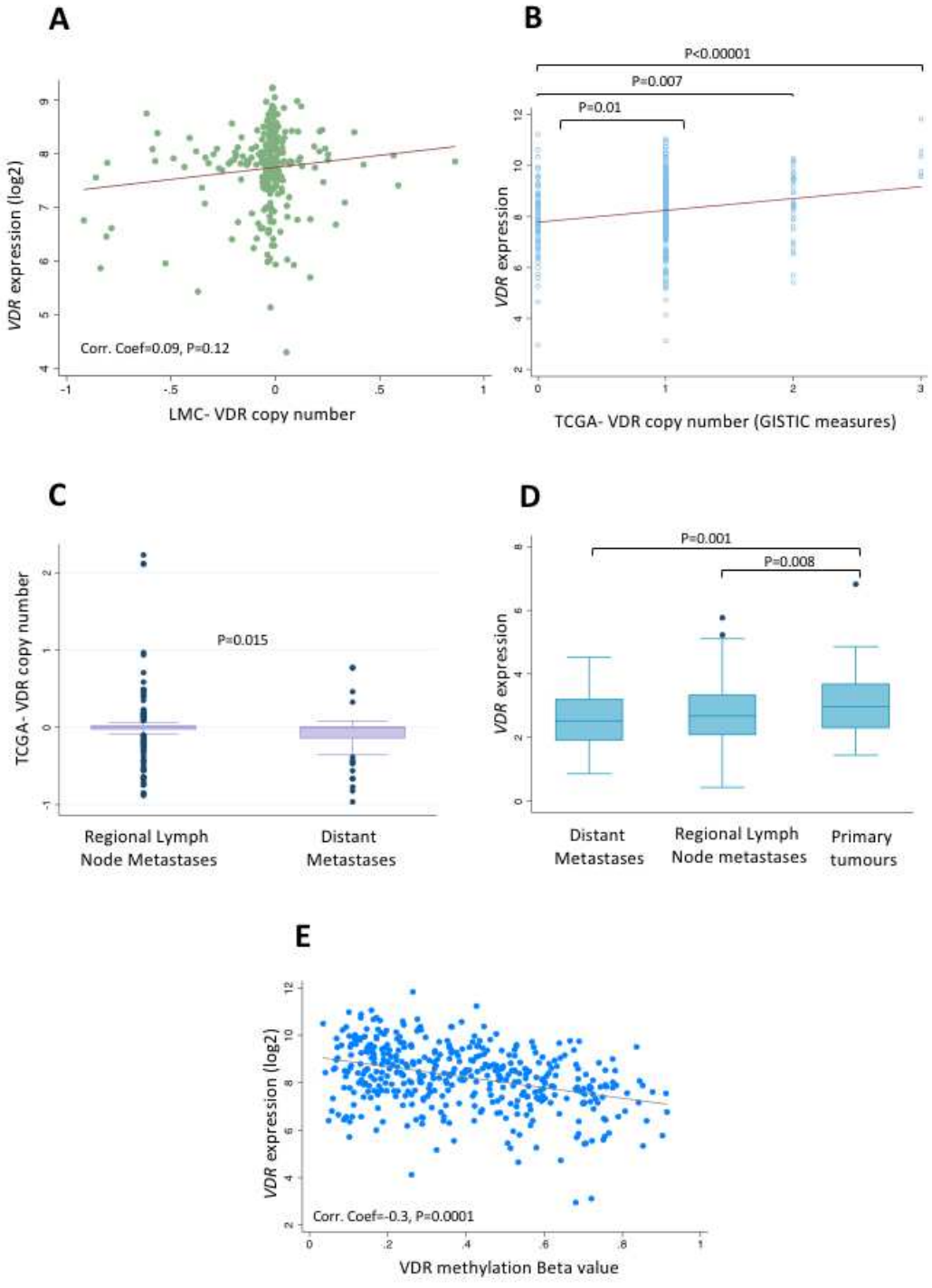
A
VDR expression (log2)
Corr. Coef=0.09, P=0.12
LMC- VDR copy number
B
P<0.00001
P=0.007
P=0.01
VDR expression
TCGA- VDR copy number (GISTIC measures)
C
TCGA- VDR copy number
P=0.015
Regional Lymph Node Metastases
Distant Metastases
D
P=0.001
P=0.008
VDR expression
Distant Metastases
Regional Lymph Node metastases
Primary tumours
E
VDR expression (log2)
Corr. Coef=-0.3, P=0.0001
VDR methylation Beta value

Figure 2

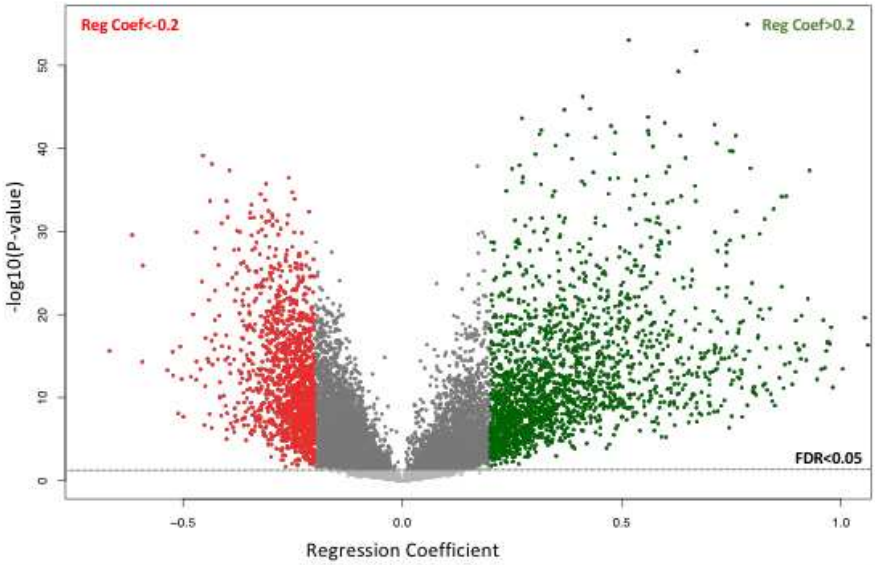

GeneSet	FDR
Cadherin signaling pathway(P)	1.82E-04
Wnt signaling pathway(P)	1.09E-03
Meiotic recombination(R)	2.75E-03
Fanconi anemia pathway(N)	3.43E-03
Mitochondrial translation(R)	5.62E-03
SRP-dependent cotranslational protein targeting to membrane(R)	5.62E-03
Assembly of the primary cilium(R)	5.81E-03
Cell cycle(K)	5.81E-03
Mitotic G1-G1/S phases(R)	0.0212
Mitotic G2-G2/M phases(R)	0.0212
Mitotic Metaphase and Anaphase(R)	0.0212
Fanconi anemia pathway(K)	0.0217
Mitotic Prometaphase(R)	0.0222
Processing of Capped Intron-Containing Pre-mRNA(R)	0.0222
SUMOylation(R)	0.0222
HDR through Homologous Recombination (HR) or Single Strand Annealing (SSA)(R)	0.0222
Ribosome(K)	0.0251
Regulation of nuclear SMAD2/3 signaling(N)	0.0371
Generic Transcription Pathway(R)	0.0371
Processing of Capped Intronless Pre-mRNA(R)	0.0396
mTOR signaling pathway(N)	0.0402
Cell Cycle Checkpoints(R)	0.0405
ATR signaling pathway(N)	0.0413

GeneSet	FDR
Extracellular matrix organization(R)	2.28E-14
Staphylococcus aureus infection(K)	2.28E-14
Cytokine-cytokine receptor interaction(K)	2.28E-14
Hematopoietic cell lineage(K)	2.28E-14
Cell adhesion molecules (CAMs)(K)	2.73E-13
Osteoclast differentiation(K)	5.44E-12
Graft-versus-host disease(K)	7.35E-12
Costimulation by the CD28 family(R)	7.35E-12
Interferon gamma signaling(R)	1.04E-11
Inflammatory bowel disease (IBD)(K)	1.26E-11
IL12-mediated signaling events(N)	1.53E-11
Tuberculosis(K)	1.71E-11
Intestinal immune network for IgA production(K)	7.66E-11
Type I diabetes mellitus(K)	8.25E-11
Rheumatoid arthritis(K)	1.32E-10
Allograft rejection(K)	2.29E-10
TCR signaling in naïve CD4+ T cells(N)	4.96E-10
TNF signaling pathway(K)	1.27E-09
Antigen processing and presentation(K)	1.90E-09
Leishmaniasis(K)	2.06E-09
Pathways in cancer(K)	2.46E-09
Phagosome(K)	2.72E-09
Viral myocarditis(K)	2.99E-09
NF-kappa B signaling pathway(K)	3.13E-09
T cell receptor signaling pathway(K)	3.76E-09

Figure 3

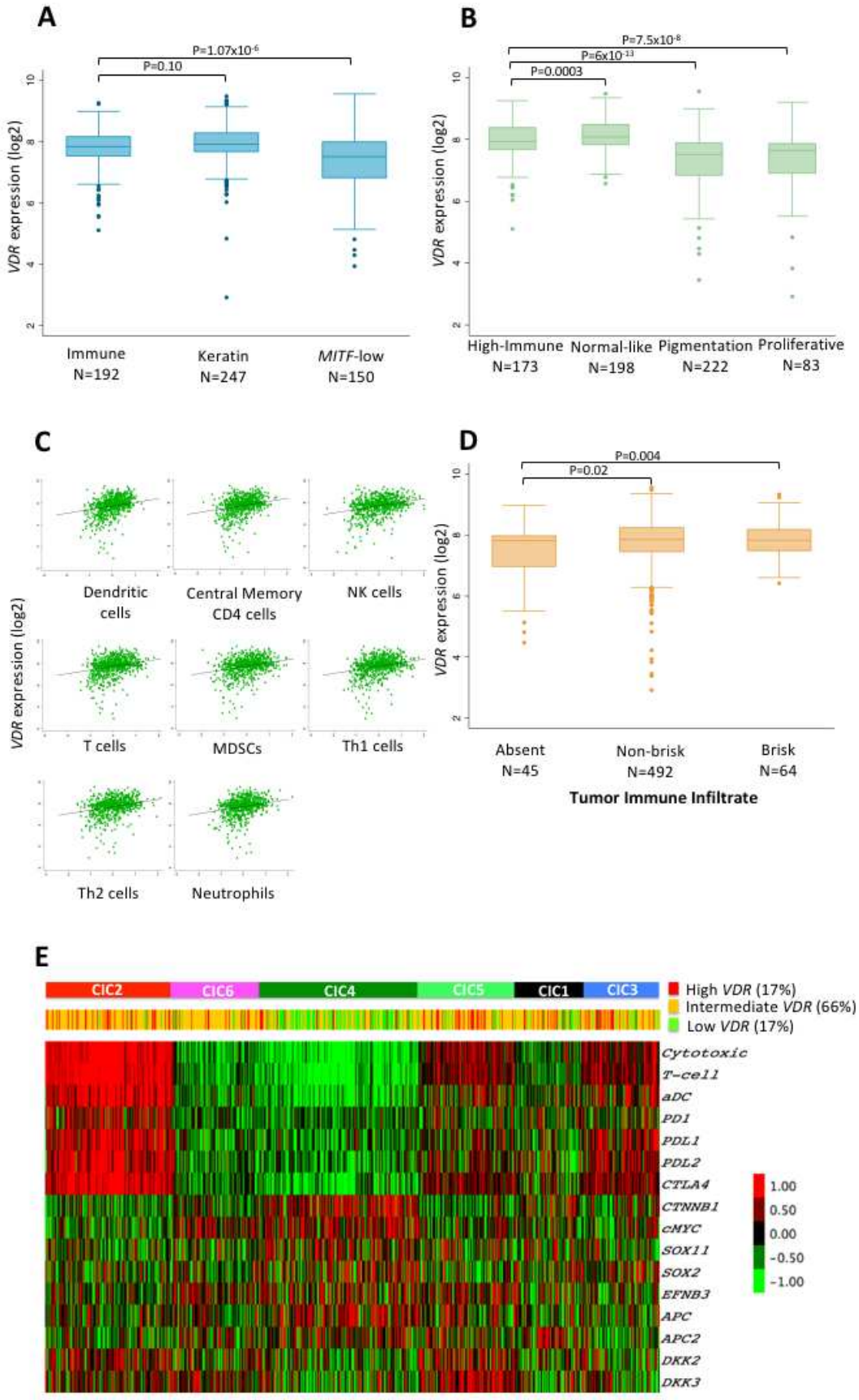
A
P=1.07x10-6
P=0.10
VDR expression (log2)
Immune N=192
Keratin N=247
MITF-low N=150
B
P=7.5x10-8
P=6x10-13
P=0.0003
VDR expression (log2)
High-Immune N=173
Normal-like N=198
Pigmentation N=222
Proliferative N=83
C
VDR expression (log2)
Dendritic cells
Central Memory CD4 cells
NK cells
T cells
MDSCs
Th1 cells
Th2 cells
Neutrophils
D
P=0.004
P=0.02
VDR expression (log2)
Absent N=45
Non-brisk N=492
Brisk N=64
Tumor Immune Infiltrate
E
CIC2
CIC6
CIC4
CIC5
CIC1
CIC3
High VDR (17%)
Intermediate VDR (66%)
Low VDR (17%)
Cytotoxic
T-cell
aDC
PD1
PDL1
PDL2
CTLA4
CTNNB1
cMYC
SOX11
SOX2
EFNB3
APC
APC2
DKK2
DKK3
1.00
0.50
0.00
-0.50
-1.00

Figure 4

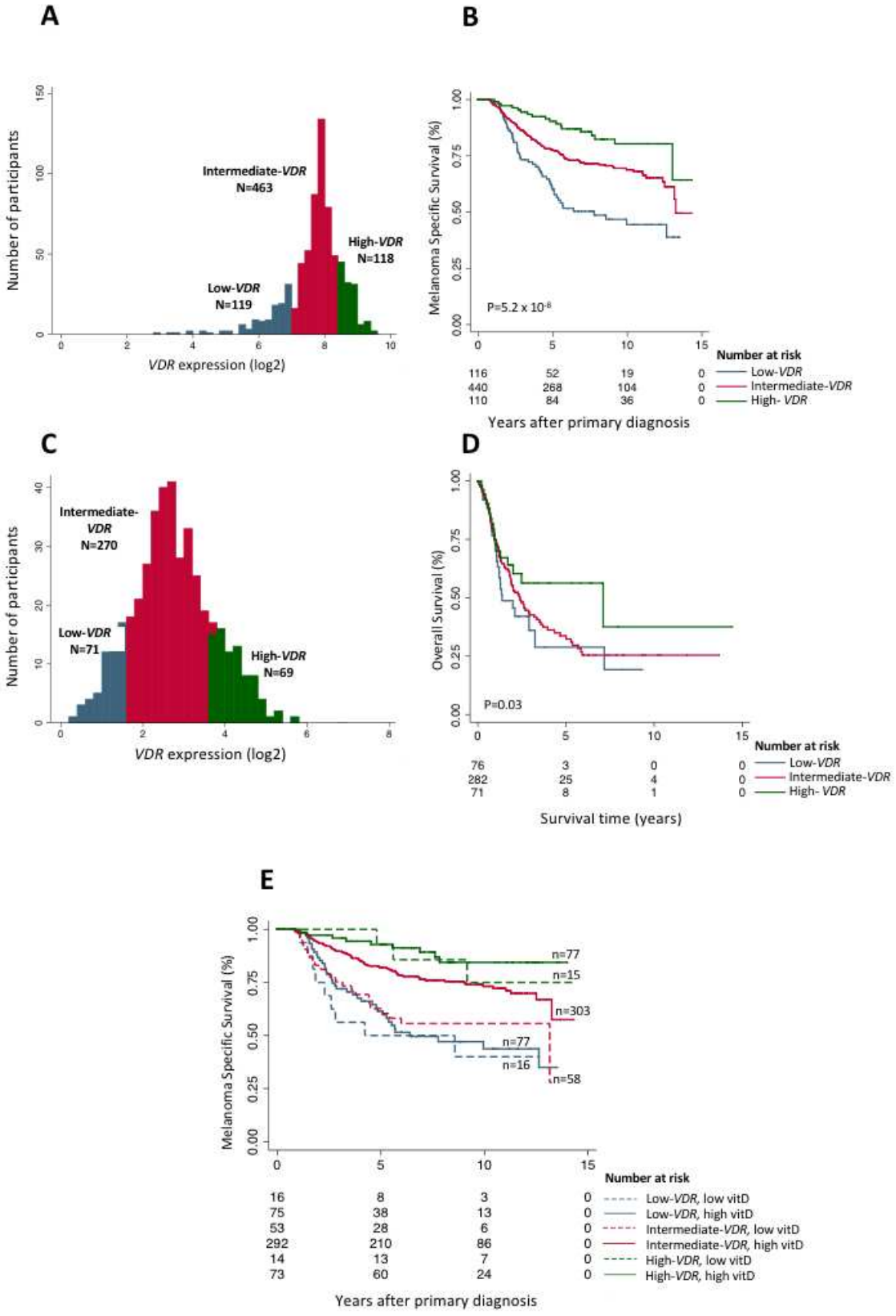
A
Number of participants
Intermediate-VDR
N=463
High-VDR
N=118
Low-VDR
N=119
VDR expression (log2)
B
Melanoma Specific Survival (%)
P=5.2 x 10-8
Number at risk
Low-VDR
Intermediate-VDR
High- VDR
116 52 19 0
440 268 104 0
110 84 36 0
Years after primary diagnosis
C
Number of participants
Intermediate-VDR
N=270
Low-VDR
N=71
High-VDR
N=69
VDR expression (log2)
D
Overall Survival (%)
P=0.03
Number at risk
Low-VDR
Intermediate-VDR
High- VDR
76 3 0 0
282 25 4 0
71 8 1 0
Survival time (years)
E
Melanoma Specific Survival (%)
n=77
n=15
n=303
n=77
n=16
n=58
Number at risk
Low-VDR, low vitD
Low-VDR, high vitD
Intermediate-VDR, low vitD
Intermediate-VDR, high vitD
High-VDR, low vitD
High-VDR, high vitD
16 8 3 0
75 38 13 0
53 28 6 0
292 210 86 0
14 13 7 0
73 60 24 0
Years after primary diagnosis

Figure 5

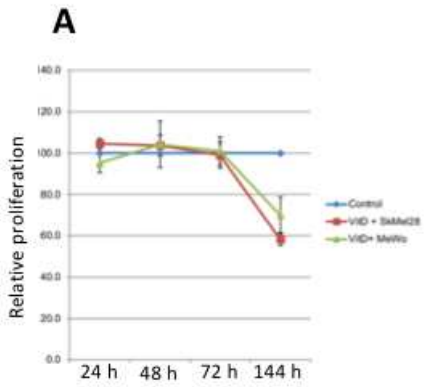
A
Relative proliferation
140.0
120.0
100.0
80.0
60.0
40.0
20.0
0.0
24 h
48 h
72 h
144 h
Control
VID + SkMel28
VID+ MeWo

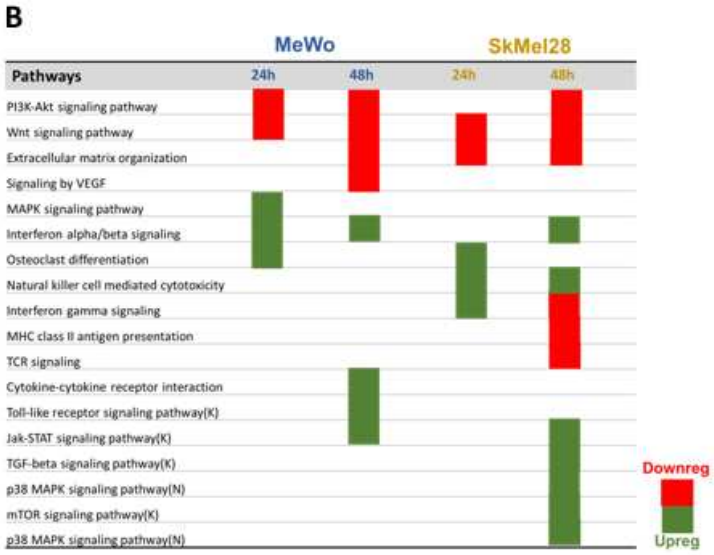
B
MeWo
SkMel28
Pathways
24h
48h
24h
48h
PI3K-Akt signaling pathway
Wnt signaling pathway
Extracellular matrix organization
Signaling by VEGF
MAPK signaling pathway
Interferon alpha/beta signaling
Osteoclast differentiation
Natural killer cell mediated cytotoxicity
Interferon gamma signaling
MHC class II antigen presentation
TCR signaling
Cytokine-cytokine receptor interaction
Toll-like receptor signaling pathway(K)
Jak-STAT signaling pathway(K)
TGF-beta signaling pathway(K)
p38 MAPK signaling pathway(N)
mTOR signaling pathway(K)
p38 MAPK signaling pathway(N)
Downreg
Upreg

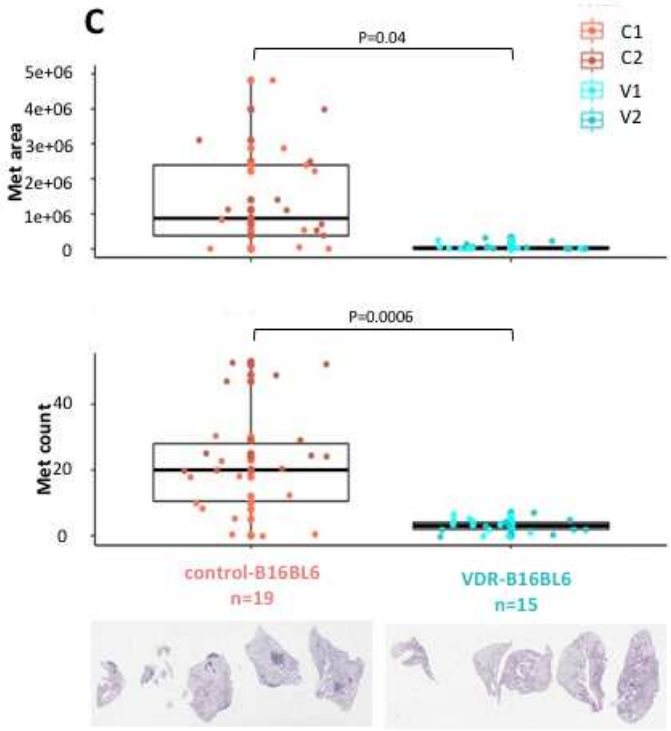
C
P=0.04
C1
C2
V1
V2
Met area
5e+06
4e+06
3e+06
2e+06
1e+06
0
P=0.0006
Met count
40
20
0
control-B16BL6
n=19
VDR-B16BL6
n=15

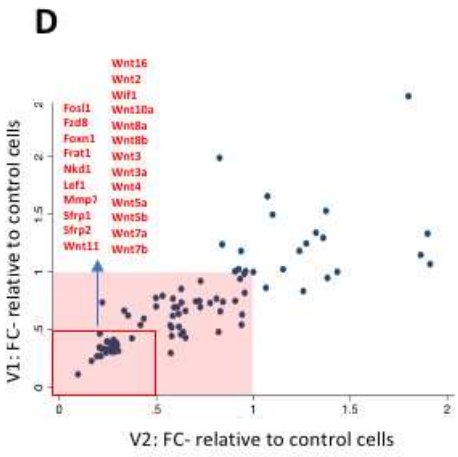
D
Wnt16
Wnt2
Wif1
Wnt10a
Wnt8a
Wnt8b
Wnt3
Wnt3a
Wnt4
Wnt5a
Wnt5b
Wnt7a
Wnt7b
Fosl1
Fzd8
Foxn1
Frat1
Nkd1
Lef1
Mmp7
Sfrp1
Sfrp2
Wnt11
V1: FC- relative to control cells
V2: FC- relative to control cells
0
.5
1
1.5
2